^{18}F-FDG PET/MRI Can Be Used to Identify Injured Peripheral Nerves in a Model of Neuropathic Pain

Deepak Behera, Kathleen E. Jacobs, Subrat Behera, Jarrett Rosenberg, and Sandip Biswal

Department of Radiology, Molecular Imaging Program at Stanford, Stanford University, California

We demonstrated increased ^{18}F-FDG uptake in injured peripheral nerves in a model of neuropathic pain using small-animal PET/MRI. **Methods:** A neuropathic pain model in rats was created by spared-nerve injury of the left sciatic nerve. Sham-operated rats without nerve injury were used as a control. The presence of pain was confirmed by testing for allodynia. Sequential small-animal ^{18}F-FDG PET and MRI scans of the thighs were obtained and coregistered. Autoradiography was performed on harvested nerves and muscle. **Results:** The group with spared-nerve injury showed the development of allodynia in the operated limb ($P < 0.001$). Increased ^{18}F-FDG uptake was observed on both PET/MRI ($P < 0.001$) and autoradiography ($P < 0.005$) in the operated nerve in this group. ^{18}F-FDG uptake in the nerves correlated well with allodynia ($\rho = -0.59$; $P < 0.024$). **Conclusion:** Animals with neuropathic pain show increased ^{18}F-FDG uptake in the affected nerve. Small-animal PET/MRI can be effectively used to localize ^{18}F-FDG uptake in peripheral nerves.

Key Words: PET/MRI; neuropathic pain; ^{18}F-FDG; spared nerve injury

J Nucl Med 2011; 52:1308–1312
DOI: 10.2967/jnumed.110.084731

Increased spontaneous activity (*1*) and metabolic changes (*2,3*) are known to occur in injured nerves and are largely attributed to the symptoms of neuropathic pain. Neuronal activity is dependent on glucose metabolism (*4*). Isolated cases of increased ^{18}F-FDG uptake in peripheral nerves have been reported in noncancerous cases of peripheral neuropathy and neural inflammation (*5,6*). Little is known about glucose metabolism in the peripheral nervous system using ^{18}F-FDG in the setting of noncancerous nerve injury. To our knowledge, this study was the first systematic study of ^{18}F-FDG uptake in the peripheral nerves in a noncancerous setting, specifically in a rat model of neuropathic pain. Furthermore, we demonstrated the utility of coregistered MRI in localizing metabolic activity in peripheral nerves.

Received Oct. 28, 2010; revision accepted Apr. 4, 2011.
For correspondence or reprints contact: Sandip Biswal, 300 Pasteur Dr., S-062B, Stanford, CA 94305.
E-mail: biswal@stanford.edu.

MATERIALS AND METHODS

Neuropathic Pain Model

Animal experiments were approved by the institutional animal care and use committee. Two groups of male adult Sprague–Dawley rats weighing 200–250 g were used. The first was the spared-nerve injury group ($n = 3$), which underwent a left spared-nerve injury procedure that creates a well-characterized neuropathic pain model (*7*). Briefly, under aseptic surgical techniques and inhalational 2%–3% isoflurane anesthesia, the left sciatic nerve and its 3 terminal branches were surgically accessed. A ligation and axotomy of the tibial and common peroneal nerves was performed, sparing the sural nerve. The second group was a control group ($n = 3$), which was subjected to a sham operation similar to that used on the spared-nerve injury animals but without the nerve injury. Animals were permitted to heal for 4 wk after the surgery.

Pain Behavior Assessment

Allodynia, a common feature of neuropathic pain, is pain that results from a stimulus that would normally not provoke pain. Development of mechanical allodynia was evaluated during the third week after surgery using von Frey hair filaments. Animals were acclimatized on a raised wire-mesh platform for 2 h/d for 4 d before testing and an hour just before testing. The filament was applied to the lateral portion of the plantar aspect of both hind paws through the mesh floor and pressed until it bent, and then kept in place for 8 s. A brisk withdrawal of the paw was considered a positive response, which was confirmed with the same filament again after at least 60 s. The testing endpoint was 3 consecutive positive responses for the same filament or if the filament lifted the paw off the floor. The data thus collected were analyzed using the PsychoFit software program (http://psych.colorado.edu/~lharvey/html/software.html), which calculates the 50% withdrawal threshold in log filament stiffness units. The threshold is defined as the stimulus intensity at which the withdrawal is detected 50% of the time (*8,9*).

Small-Animal PET/MRI

All animals were anesthetized with humidified 2%–3% isoflurane throughout imaging. Longitudinal fiducial markers containing dilute tracer solution (1.3 MBq/mL) were fixed to the animal holder. The animal was rigidly secured in a transportable holder to minimize motion while being transferred between the PET and MRI scanners. The animals underwent sequential small-animal PET (microPET R4; Siemens Medical Solutions) and small-animal MRI (a self-shielded 30-cm-bore 7-T magnet [Varian] with a 9-cm-bore gradient insert [Resonance Research Inc.] using EXCITE2 electronics and the supporting LX11 platform; GE Healthcare]. For the PET scan, 18.5 MBq of ^{18}F-FDG were injected intravenously and the

TABLE 1
Withdrawal Threshold Data for Right and Left Hind Paws Before and After Surgery

Group	Baseline		Postsurgery	
	Left	Right	Left	Right
Spared-nerve injury				
Mean log stiffness units	5.38	5.27	4.72*	5.52
SD log stiffness units	0.24	0.07	0.16	0.37
n	3	3	3	3
Control				
Mean log stiffness units	5.07	5.02	5.00	5.00
SD log stiffness units	0.05	0.10	0.05	0.07
n	3	3	3	3

*$P < 0.001$.

animals were kept anesthetized on a warmed platform (35°C) for 1 h before imaging. A 10-min static scan of the thighs was obtained, after which the animals were transferred to the MRI scanner. T1-weighted fast spin-echo images (repetition time, 800 ms; echo time, 7.7 ms; slice thickness, 1 mm; in-plane resolution, 234 μm^2) were obtained of the thighs in an ambient temperature maintained at 35°C.

Autoradiography

Immediately after undergoing PET/MRI, the animals were sacrificed, and the sciatic nerves and adjacent muscles were harvested. The tissues were placed on a phosphor screen (medium MultiSensitive Phosphor Screen; PerkinElmer) and exposed for 24 h. The screen was imaged using a variable-mode imager (Typhoon 9410; GE Healthcare).

Image Analysis

The PET and MRI scans were coregistered using AMIDE image analysis software (bin 0.9.2; http://amide.sourceforge.net). The MRI images were used to define the anatomic location of the peripheral nerves and the placement of regions of interest (ROIs). Radioactivity counts were then recorded from within the ROIs in the fused PET images. The average signal from ROIs in adjacent muscle was used to normalize the maximum signal from the nerve ROIs, which were placed on 5-mm segments of sciatic nerve in each thigh, proximal to the level of injury.

Raw autoradiography images were converted to tagged image file format and analyzed using OsiriX imaging software (version 3.7.1; http://www.osirix-viewer.com/index.html). Background-subtracted maximum signal from ROIs placed around entire nerves was normalized to background-subtracted mean signal from ROIs placed within muscles.

Statistical Analysis

To test the ability to detect changes in the spared-nerve injury group, nonparametric marginal models (*10*) were estimated and the group × side interaction (or, in the case of the von Frey results, the group × side × time interaction) was tested for significance. A Bonferroni-adjusted 1-sided *P* value of 0.0125 was used as the significance level. Statistical analyses were done with R software (version 2.9.2; www.r-project.org), using version 1.2 of the "nparLD" package. Results are expressed as mean ± SD. Correlations among withdrawal thresholds by von Frey tests, ^{18}F-FDG signal with PET/MRI, and ^{18}F-FDG signal with autoradiography were calculated by Spearman rank-order correlations, and exact tests were done to assess their statistical significance using a 1-sided *P* value of 0.05. A single tie in von Frey scores was broken in favor of the null hypothesis.

RESULTS

Animals with Spared-Nerve Injury Exhibit Allodynia

Development of allodynia, assessed using the von Frey hair test, was seen only in the spared-nerve injury group

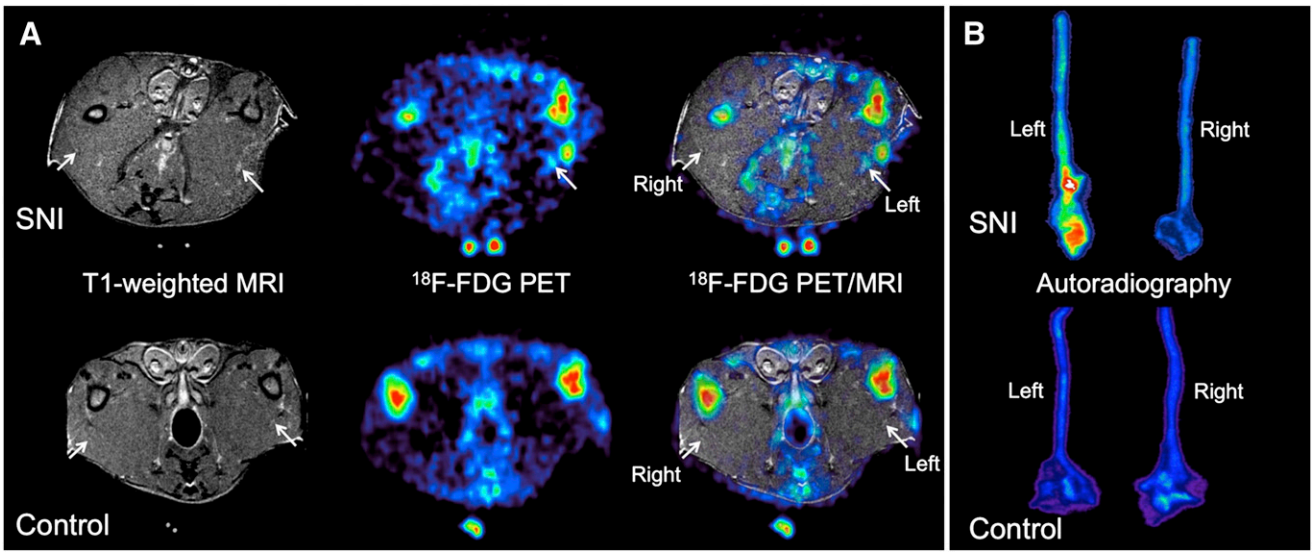

FIGURE 1. Representative spared-nerve injury (top row) and control (bottom row) animals showing sciatic nerves (arrows) on transaxial MRI, PET, and PET/MRI (A) and autoradiography of excised sciatic nerves (B). On ^{18}F-FDG PET/MRI, significantly increased normalized ^{18}F-FDG uptake is seen on side with spared-nerve injury (left), compared with control side (right). Control animals did not show any significant difference between right and left nerves. Autoradiography of sciatic nerve specimens from spared-nerve injury animals showed that normalized radiotracer uptake is higher in injured sciatic nerve (left) than in control sciatic nerve (right). Control animals did not show any significant difference between right and left nerves. SNI = spared-nerve injury.

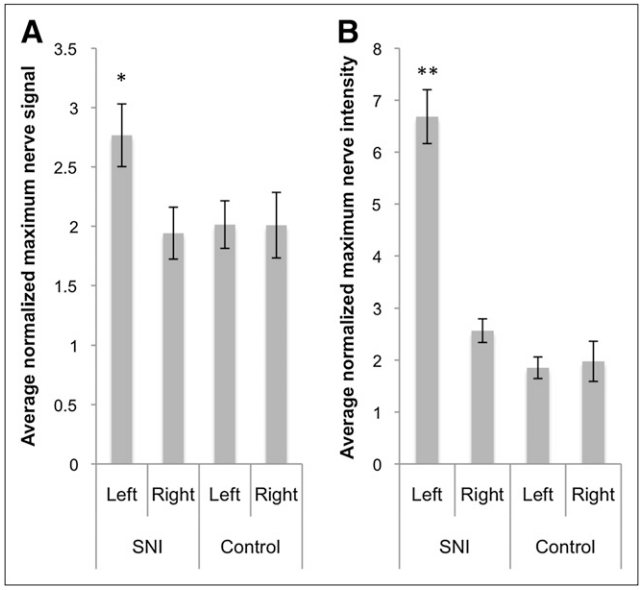

FIGURE 2. Average normalized maximum signal in sciatic nerves on PET/MRI (A) and autoradiography (B). Error bars represent SE of mean. On both PET/MRI and autoradiography, greater ^{18}F-FDG uptake is seen in left nerve of spared-nerve injury group than in right nerve of spared-nerve injury group or in either nerve of control group. SNI = spared-nerve injury. *$P < 0.001$. **$P < 0.005$.

(Table 1). Lower withdrawal thresholds were seen in the left hind limb of the spared-nerve injury group after surgery than before surgery (in log stiffness units, 5.38 ± 0.24 at baseline and 4.72 ± 0.16 after surgery; $P < 0.001$). No change in withdrawal thresholds was observed after surgery in the right hind limb of the spared-nerve injury group or in either hind limb of the control group.

Sciatic Nerves with Spared-Nerve Injury Show Increased ^{18}F-FDG Uptake on PET/MRI

On the coregistered PET/MRI scans, increased tracer uptake was visualized in the injured sciatic nerve in animals with spared-nerve injury (Fig. 1A). Significantly higher normalized maximum ^{18}F-FDG uptake was found in the left sciatic nerve of the spared-nerve injury group (2.77 ± 0.46, $P < 0.001$) than in the right sciatic nerve of that group (1.94 ± 0.38) or in either sciatic nerve of the control group (left, 2.01 ± 0.35; right, 2.01 ± 0.48) (Fig. 2A).

Sciatic Nerves with Spared-Nerve Injury Show Increased ^{18}F-FDG Uptake on Autoradiography

After PET/MRI, both sciatic nerves were harvested from each animal for autoradiography. Significantly increased normalized maximum ^{18}F-FDG uptake was seen in the left sciatic nerve of the spared-nerve injury group, especially in the neuroma at the site of transection (6.68 ± 0.90, $P < 0.005$) (Fig. 1B), compared with the right sciatic nerve of that group (2.57 ± 0.39) or either sciatic nerve of the control group (left, 1.85 ± 0.36; right, 1.98 ± 0.67) (Fig. 2B).

Correlation of ^{18}F-FDG Uptake Is Observed in Nerves and Pain Behavior

A good correlation was observed between ^{18}F-FDG uptake on PET/MRI (normalized maximum signal in left and right nerves) and behavioral measurements (withdrawal threshold in right and left hind paws) of spared-nerve injury and control animals ($\rho = -0.59$, $n = 12$, $P = 0.024$). Lower withdrawal thresholds (increased pain sensitivity) correlated with higher normalized ^{18}F-FDG uptake in the nerves. A similar negative correlation, which was not significant, was seen between ^{18}F-FDG uptake on autoradiography and behavioral measurements ($\rho = -0.42$, $n = 12$, $P = 0.088$). ^{18}F-FDG uptake on PET/MRI and autoradiography was well correlated ($\rho = 0.72$, $n = 12$, $P = 0.006$) (Fig. 3).

Increased ^{18}F-FDG Uptake Is Observed in Ipsilateral Calf Tissues of Spared-Nerve Injury Animals

Interestingly, significantly increased soft-tissue uptake of ^{18}F-FDG was seen in the calf tissues of spared-nerve injury

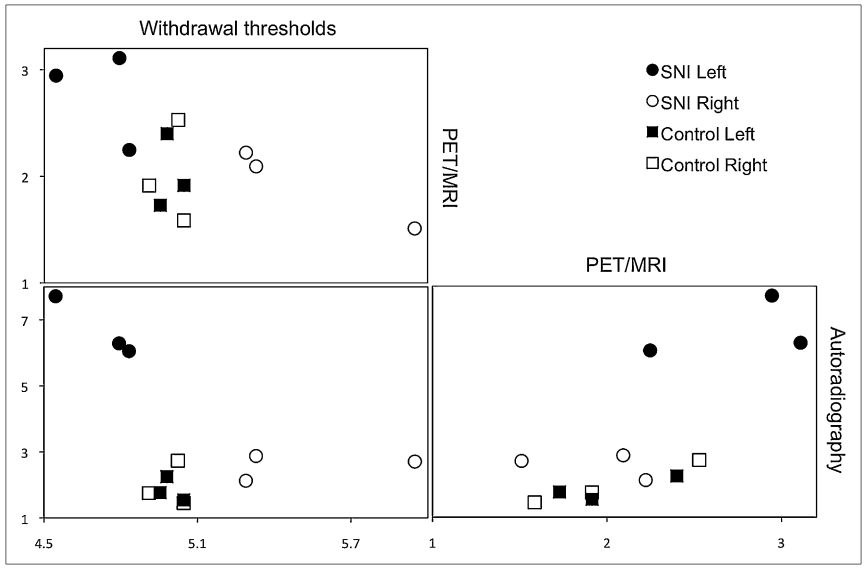

FIGURE 3. Scatterplots between withdrawal thresholds on von Frey testing, normalized ^{18}F-FDG uptake on PET/MRI, and normalized ^{18}F-FDG uptake on autoradiography as seen on left and right sides of spared-nerve injury and control groups. SNI = spared-nerve injury.

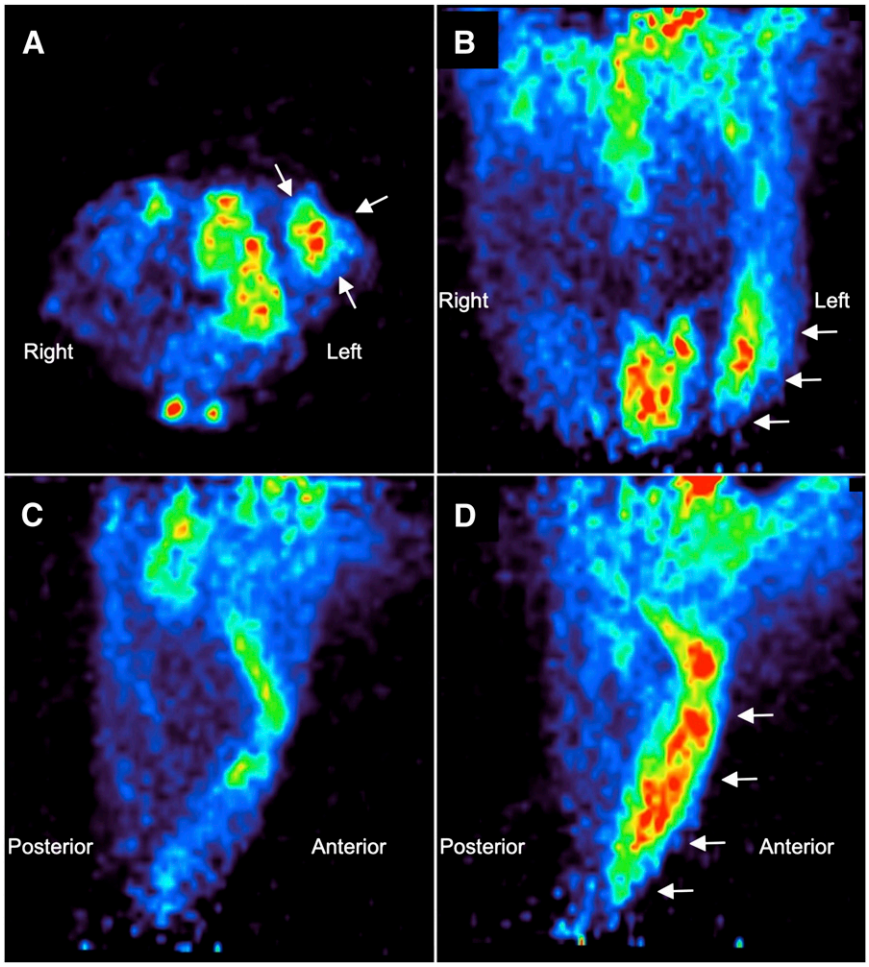

FIGURE 4. Increased soft-tissue uptake of ^{18}F-FDG in ipsilateral calf of spared-nerve injury animals. PET images were acquired of representative spared-nerve injury animal through its hind limbs: transaxial section (A), coronal section (B), sagittal section through right hind limb (C), and sagittal section through left hind limb (D). Arrows point to soft tissue with visibly increased ^{18}F-FDG uptake in left hind limb.

animals on the same side as the injured nerve (Fig. 4). Because we had not anticipated such an observation, we did not include the distal parts of the hind limbs in the MRI scans. Cylindric ROIs (3 × 5 mm) were placed on the calf, carefully avoiding the tibiae, in all PET images. The mean signal in these ROIs was normalized to the mean muscle signal in the thigh muscles. Increased ^{18}F-FDG uptake was seen in the calf soft tissues on the side ipsilateral to the nerve injury in the spared-nerve injury group (5.59 ± 1.62, $P < 0.001$), compared with the contralateral calf in the spared-nerve injury group (1.95 ± 0.67) or either calf in the control group (left, 1.75 ± 0.31; right, 1.89 ± 0.38).

DISCUSSION

Increased cellular metabolism and glucose utilization can be observed in injured nerves. These observations may be due to increased spontaneous firing in pain-sensing neurons (*2,3,11*) and may be part of a neuronal response to nerve injury, including neuronal stress and nerve regenerative processes such as axonal sprouting and protein synthesis (*12*). ^{18}F-FDG is a well-established metabolic activity marker using PET and, by extension, can be considered a marker for increased neuronal activity in the setting of nerve injury and neuropathic pain.

^{18}F-FDG has already been used to study neuronal metabolic activity changes in the cerebrum (*13–15*) and specifically in relation to chronic pain (*16*). To our knowledge, this study was the first to address nociception-related ^{18}F-FDG uptake in peripheral nerves. Metabolic imaging of peripheral nociception has been challenged by the relatively poor spatial resolution of small-animal PET, which varies from 0.7 to 1.84 mm in full width at half maximum in phantom studies (*17*) (the sciatic nerve is 1–2 mm thick in rats), and the difficulty in distinguishing peripheral nerves from background activity using PET alone.

Because of their better spatial resolution, CT and MRI have been established as anatomic localization tools with PET. By coregistering images from 2 modalities, we were able to use the excellent spatial and contrast resolution of MRI to locate sciatic nerves and then use ^{18}F-FDG PET to observe metabolic changes in them associated with nerve injury.

In this study, increased ^{18}F-FDG uptake was seen in neuropathic nerves. The radiotracer uptake detected with PET/MRI correlated well with that seen on autoradiography, both of which also correlated well with pain behaviors. Although the correlations were driven by the small number of pain responses (Fig. 3), they demonstrated the mutual

consistency of ^{18}F-FDG uptake measurements in the nerves by PET/MRI and autoradiography.

Incidentally, increased ^{18}F-FDG was seen in the gastrocnemius muscles of the calf on the side of nerve injury in spared-nerve injury animals (Fig. 4). On reviewing the literature for an explanation, we found that Handberg et al. reported, in sciatic nerve transections, an increase in basal glucose transport in the denervated calf muscles (*18*).

CONCLUSION

PET/MRI can potentially be used as a tool to image and evaluate peripheral neural diseases. Using MRI guidance, subtle changes in tissue metabolism can be appreciated within discrete soft-tissue structures that would not be otherwise possible using PET only or CT. Considering the small sizes and similar densities of various tissues and organs in small animals, small-animal PET/MRI can potentially serve as a valuable preclinical tool.

DISCLOSURE STATEMENT

The costs of publication of this article were defrayed in part by the payment of page charges. Therefore, and solely to indicate this fact, this article is hereby marked "advertisement" in accordance with 18 USC section 1734.

ACKNOWLEDGMENTS

We thank Dr. David Dick and his colleagues for the production of ^{18}F-FDG in the Cyclotron Radiochemistry Facility, and Drs. Laura Pisani, Timothy Doyle, and Aileen Hoehne for assistance with the small-animal imaging devices and autoradiography in the Small Animal Imaging Facility at Stanford University. Support was provided in part by the Weston Havens Foundation and seed funding from the Department of Radiology. No other potential conflict of interest relevant to this article was reported.

REFERENCES

1. Liu X, Eschenfelder S, Blenk KH, Janig W, Habler H. Spontaneous activity of axotomized afferent neurons after L5 spinal nerve injury in rats. *Pain.* 2000;84:309–318.
2. Ames A III. CNS energy metabolism as related to function. *Brain Res Brain Res Rev.* 2000;34:42–68.
3. Magistretti PJ, Pellerin L, Rothman DL, Shulman RG. Energy on demand. *Science.* 1999;283:496–497.
4. Barros LF, Deitmer JW. Glucose and lactate supply to the synapse. *Brain Res Rev.* 2010;63:149–159.
5. Cheng G, Chamroonrat W, Bing Z, Huang S, Zhuang H. Elevated FDG activity in the spinal cord and the sciatic nerves due to neuropathy. *Clin Nucl Med.* 2009;34:950–951.
6. Bertagna F, Giubbini R, Biasiotto G, Rosenbaum J, Alavi A. Incidental inflammatory findings in nerves and in patients with neoplastic diseases evaluated by ^{18}F-FDG-PET/CT. *Hell J Nucl Med.* 2009;12:279–280.
7. Decosterd I, Woolf CJ. Spared nerve injury: an animal model of persistent peripheral neuropathic pain. *Pain.* 2000;87:149–158.
8. Berquin AD, Lijesevic V, Blond S, Plaghki L. An adaptive procedure for routine measurement of light-touch sensitivity threshold. *Muscle Nerve.* 2010;42:328–338.
9. Gescheider GA. *Psychophysics Method, Theory, and Application.* 2nd ed. Hillsdale, NJ: Lawrence Erlbaum Associates; 1985.
10. Brunner E, Domhof S, Langer F. *Nonparametric Analysis of Longitudinal Data in Factorial Experiments.* New York, NY: John Wiley and Sons; 2002.
11. Magistretti PJ. Neuroscience: low-cost travel in neurons. *Science.* 2009;325:1349–1351.
12. Kreutzberg GW. Principles of neuronal regeneration. *Acta Neurochir Suppl.* 1996;66:103–106.
13. Chen YY, Shih YY, Lo YC, et al. MicroPET imaging of noxious thermal stimuli in the conscious rat brain. *Somatosens Mot Res.* 2010;27:69–81.
14. Kulkarni B, Bentley DE, Elliott R, et al. Arthritic pain is processed in brain areas concerned with emotions and fear. *Arthritis Rheum.* 2007;56:1345–1354.
15. Ohashi K, Ichikawa K, Chen L, Callahan M, Zasadny K, Kurebayashi Y. MicroPET detection of regional brain activation induced by colonic distention in a rat model of visceral hypersensitivity. *J Vet Med Sci.* 2008;70:43–49.
16. Buvanendran A, Ali A, Stoub TR, Kroin JS, Tuman KJ. Brain activity associated with chronic cancer pain. *Pain Physician.* 2010;13:E337–E342.
17. Weber S, Bauer A. Small animal PET: aspects of performance assessment. *Eur J Nucl Med Mol Imaging.* 2004;31:1545–1555.
18. Handberg A, Megeney LA, McCullagh KJ, Kayser L, Han XX, Bonen A. Reciprocal GLUT-1 and GLUT-4 expression and glucose transport in denervated muscles. *Am J Physiol.* 1996;271:E50–E57.